Can Hydrocarbon Chains Be Disrupted by Fast O(3P) Atoms?

Asta Gindulytė and Lou Massa*

Department of Chemistry, Hunter College, 695 Park Avenue, New York, New York 10021, and The Graduate School, City University of New York, 365 Fifth Avenue, New York, New York 10016

Bruce A. Banks and Sharon K. Rutledge

NASA Glenn Research Center, 21000 Brookpark Road, M/S 309-2, Cleveland, Ohio 44135

Received: May 17, 2000; In Final Form: August 30, 2000

O(3P) is a highly reactive species which may cause damage to materials on contact. In low Earth orbit (LEO), high-energy collisions (∼4.5 eV) of O(3P) with spacecraft materials can lead to extensive degradation. In this study, we use ab initio molecular orbital calculations to investigate the possibility of chain breaking in polyethylene caused by a single O(3P) attack under LEO conditions, because the occurrence of such reactions could greatly accelerate the erosion. The smallest alkanes ($n = 2$, 3, 5, or 7) serve as models of polyethylene. For the case of ethane ($n = 2$), we explore the triplet potential energy surface of the following reaction: $O(3P) + CH_3{-}CH_3 \rightarrow {\cdot}O{-}CH_3 + {\cdot}CH_3$. Analogous reactions, in which O(3P) attacks a central carbon atom, are studied for the higher alkanes. Results obtained using the Hartree−Fock method, density functional theory, and, in the simplest case (i.e., ethane), second-order Möller−Plesset perturbation theory, Gaussian theoretical models (G1, G2, and G2MP2), and complete basis set (CBS-QB3) approaches are reported. We conclude that conditions in LEO are conducive to chain breaking in polyethylene caused by a single O(3P) attack.

Introduction

The space shuttle, the international space station (ISS), and many other satellites travel around the Earth through the space region called low Earth orbit (LEO), the altitudes of 180−650 km above the Earth's surface. The largest component of the atmosphere[1] at these altitudes is atomic oxygen (AO), which is created when oxygen molecules are split by short wavelength solar ultraviolet radiation in an environment where the mean free path is sufficiently large that the probability of recombination is negligible. The typical O-atom number density at space shuttle altitudes is on the order of 10^8 cm^{-3}. A LEO orbiting body typically travelling at 7.2 km/s relative to this density experiences a flux of 10^{14} O-atoms/(cm^2 s). Oxygen atoms hit the spacecraft surface with impact energies of approximately 4.5 eV (∼100 kcal/mol).[2] Exposure to harsh LEO environment leads to significant changes in the condition of many spacecraft surface materials. Materials particularly affected by LEO are organic polymers which lose weight and, depending on thickness, can be eroded away completely.[3−10]

Knowledge of the long-term durability of materials exposed to AO in the LEO environment is crucial to numerous space missions and experiments. In addition to space shuttle flights, the effects of AO interaction with various materials have been studied at ground-based laboratory facilities.[1,11−19] The erosion yield of materials may be influenced by factors such as AO flux, AO fluence, synergistic solar radiation, AO impact energy, AO impact angle, material temperature, and so forth. Phenomenological models have been developed to explain observed trends in materials degradation.[20] However, despite the research that has been done, to date there is no clear understanding of elementary reaction mechanisms for materials interaction with AO.

* To whom correspondence should be addressed. Fax: 212-772-5332. E-mail: lmassa@hunter.cuny.edu.

Although a material consisting entirely of long aliphatic hydrocarbon chains, polyethylene, is not extensively used as spacecraft surface material, there are reasons for understanding its erosion by AO mechanism. First, it has a simple chemical structure, and therefore it would seem that the degradation mechanisms would have to be among the simplest ones to study. Second, there are quite a few materials that are used or are being considered for use in spacecraft surface applications that contain fragments of type $(CH_2)_n$ ($n \geq 1$) in their polymer repeat units.

LEO observed erosion rates for polyethylene are among the highest for all organic polymers (∼3.7×10^{-24} cm^3/O-atom).[8] Tests conducted at ground-based facilities showed that a low-energy AO environment produces erosion rates orders of magnitude lower than those observed in space flights, whereas the erosion rates measured in fast AO beams are close to those observed in space.[17−19]

Hydrogen abstraction reactions are well-known between hydrocarbons and atomic oxygen in its ground state, O(3P). Moreover, it is usually assumed that hydrogen abstraction is the only type of reaction that would take place between saturated hydrocarbons and O(3P). However, given the unusual LEO conditions, for example, oxygen atoms hitting the surface of polyethylene with impact energies ∼100 kcal/mol, a possibility exists that O(3P) attacks on carbon−carbon bonds, resulting in the breaking of polymer chains, could occur. In this work, we use ab initio techniques to investigate the reaction of O(3P) attack on carbon−carbon bonds of ethane and several higher alkanes, which we consider to be models, however simple, of polyethylene.

Computational Details

Quantum mechanical calculations were carried out with the Gaussian 98[21] and Mulliken[22] (used only for Hartree−Fock and MB3LYP-DFT methods) program packages. Traditional Har-

10.1021/jp001817h CCC: $19.00
Published on Web 10/14/2000

TABLE 1: Structural Parameters[a] for the Transition State of the Reaction $C_2H_6 + O(3P) \rightarrow CH_3 + OCH_3$

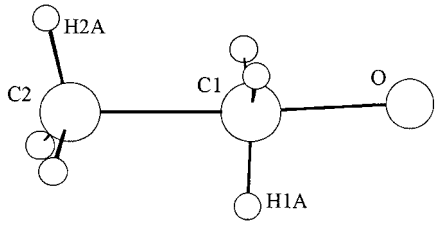

theory	r_{O-C1}	r_{C1-C2}	$a_{O-C1-C2}$	$a_{O-C1-H1A}$	$a_{C1-C2-H2A}$
HF/3-21G	2.005	2.372	178.7	92.4	99.6
HF/6-31G(d,p)	2.157	2.488	178.9	91.2	99.1
MP2(Full)/6-31G(d)	1.723	1.920	176.6	94.2	106.0
MP2(FC)/6-31G(d,p)	1.721	1.920	176.3	94.4	105.9
MP2(FC)/6-31+G(d,p)	1.723	1.920	176.3	94.0	105.6
B3LYP/6-31G(d,p)	1.775	2.002	176.5	94.4	105.0
B3LYP/6-31+G (d,p)	1.789	2.008	176.8	93.8	104.4
B3LYP/6-311G(2d,2p)	1.782	2.005	177.1	93.7	104.4
B3LYP/6-311+G(2d,2p)	1.789	2.003	177.1	93.6	104.2
B3LYP/6-311++G(2d,2p)	1.789	2.003	177.1	93.6	104.2
B3P86/6-31+G(d,p)	1.753	1.968	176.5	94.2	105.0
B3P86/6-311+G(2d,2p)	1.754	1.963	176.7	94.0	104.7
B3PW91/6-31+G(d,p)	1.760	1.978	176.6	94.2	104.8
B3PW91/6-311+G(2d,2p)	1.759	1.972	176.8	94.0	104.6
MB3LYP/6-31+G(d,p)	1.789	2.008	176.9	93.8	104.5

[a] Bond lengths *r* in Å and bond angles *a* in deg.

tree−Fock (HF)[23−25] and second-order Möller−Plesset energy correction (MP2)[26−28] ab initio methods were used. (When calculating the relative energies for the systems in which radicals were involved, PMP2 (spin-projected MP2) rather than MP2 energies were used.) In addition, methods based on approximate procedures for estimating the "infinite correlation, infinite basis" limit were used in important test cases in order to obtain more accurate energy values. These methods were complete basis set (CBS-QB3)[29] approach and Gaussian theoretical models (G1, G2, and G2MP2).[30−33] Differing from the standard G1, G2, and G2MP2 procedure, we used zero-point energy (ZPE) values obtained with MP2 rather than HF. For anharmonicity corrections, these values were scaled by 0.9427.[34]

Several hybrid DFT methods were applied. The Becke three-parameter-hybrid (B3)[35] was used in conjunction with three correlation functionals, the Lee−Yang−Parr (LYP),[36] Perdew 86 (P86),[37,38] and Perdew−Wang 91.[39] In addition, the MB3LYP method (see ref 40) available within the Mulliken program package was used.

For all the calculations, Gaussian-type basis sets were employed (see Tables 1 and 2). The explanation and abbreviations of the basis sets can be found in ref 41.

The geometries of all reactants, products, and transition states have been optimized at the levels of theory mentioned above. For all the triplet species, that is, the transition states and O(3P), an unrestricted wave function was implemented and examined for spin contamination, which was found to be inconsequential. No symmetry constraints were imposed for optimizations of the transition states. Vibrational frequencies have been calculated using the same approximation to characterize the nature of stationary points and to determine ZPE corrections. All the stationary points have been positively identified for either minimum energy with no imaginary frequencies or for transition states with one imaginary frequency. For cases in which it was not clear (from the analysis of vibrational modes) whether a transition structure is connecting the desired reactants and products, intrinsic reaction coordinate (IRC) analysis was carried out in order to confirm that.

Computational Results

Reaction of Ethane with O(3P): $O(3P) + CH_3-CH_3 \rightarrow \cdot O-CH_3 + \cdot CH_3$. The above reaction is a methyl abstraction from ethane by O(3P). The key geometric parameters computed by ab initio and DFT methods of the transition-state structures for the ethane reaction with O(3P) are presented in Table 1. In addition, the optimized Cartesian coordinates and calculated vibrational frequencies for the transition-state structures are available in the Supporting Information. The classical and vibrational adiabatic (zero-point corrected) reaction barriers obtained by various DFT and ab initio methods are presented in Table 2.

There is no experimental evidence that suggests any information about the structure of the transition state. The appearance of this structure is very similar for all the theoretical methods used. The oxygen atom is almost aligned with the two carbon atoms. C1 and three hydrogen atoms attached to it lie in a plane, whereas C2 and its three hydrogen atoms form a pyramidal shape. A major disagreement among different methods is observed for the partially formed (O−C1) and partially broken (C1−C2) bonds of the transition-state structure. HF calculated values for the above-mentioned distances are very long as compared to those calculated by the MP2 and DFT methods. In addition, HF values obtained using a smaller basis set (3-21G) are in slightly better agreement with MP2 and DFT than those obtained using a larger basis set (6-31G(d,p)). Five different basis sets (double-ζ and triple-ζ with different numbers of polarization and diffusion functions) were used in conjunction with the B3LYP method in order to explore the effects of the various basis sets. The geometrical parameters for the transition-state structure obtained with the use of these basis sets are all very close, with the exception of the 6-31G(d,p) basis set which calculates an O−C1 bond distance of 1.775 Å as compared to 1.782−1.789 Å as obtained with the use of other basis sets. The MB3LYP method gives almost identical structural parameters as the B3LYP method. Calculations based on B3P86 and B3PW91 both produce slightly shorter distances than those

TABLE 2: Total Energies (au) and Activation Barriers (kcal/mol) for the Reaction $C_2H_6 + O(3P) \rightarrow CH_3 + OCH_3$

theory	E_{TS}	E_{C2H6}	E_O	E_a
HF/3-21G	−153.087 12	−78.793 95	−74.393 66	63.1
HF/3-21G (0 K)	−153.015 95	−78.713 89	−74.393 66	57.5
HF/6-31G(d,p)	−153.915 29	−79.238 23	−74.783 93	67.1
HF/6-31G(d,p) (0 K)	−153.845 91	−79.159 02	−74.783 93	60.9
MP2(Full)/6-31G(d)	−154.302 54	−79.503 97	−74.883 29	53.2
MP2(Full)/6-31G(d) (0 K)	−154.228 19	−79.426 77	−74.883 29	51.4
MP2(FC)/6-31G(d,p)	−154.339 62	−79.543 40	−74.881 31	53.4
MP2(FC)/6-31G(d,p) (0 K)	−154.265 08	−79.465 94	−74.881 31	51.6
MP2(FC)/6-31+G(d,p)	−154.352 42	−79.545 79	−74.886 87	50.4
MP2(FC)/6-31+G(d,p) (0 K)	−154.278 22	−79.468 80	−74.886 87	48.6
G1 (0 K)	−154.535 44	−79.624 98	−74.982 05	44.9
G2 (0 K)	−154.540 50	−79.629 32	−74.982 03	44.5
G2MP2 (0 K)	−154.534 96	−79.627 37	−74.978 68	44.6
CBS-QB3 (0 K)	−154.552 77	−79.630 58	−74.987 61	41.1
B3LYP/6-31G(d,p)	−154.835 08	−79.838 74	−75.060 62	40.3
B3LYP/6-31G(d,p) (0 K)	−154.763 02	−79.763 81	−75.060 62	38.5
B3LYP/6-31+G(d,p)	−154.848 47	−79.841 64	−75.067 61	38.1
B3LYP/6-31+G(d,p) (0 K)	−154.776 89	−79.767 04	−75.067 61	36.2
B3LYP/6-311G(2d,2p)	−154.883 99	−79.860 73	−75.085 57	39.1
B3LYP/6-311G(2d,2p) (0 K)	−154.812 16	−79.786 17	−75.085 57	37.4
B3LYP/6-311+G(2d,2p)	−154.891 00	−79.860 97	−75.090 06	37.7
B3LYP/6-311+G(2d,2p) (0 K)	−154.819 58	−79.786 46	−75.090 06	35.7
B3LYP/6-311++G(2d,2p)	−154.891 06	−79.860 98	−75.090 06	37.6
B3LYP/6-311++G(2d,2p) (0 K)	−154.819 55	−79.786 47	−75.090 06	35.8
B3P86/6-31+G(d,p)	−155.307 79	−80.168 27	−75.199 89	37.9
B3P86/6-31+G(d,p) (0 K)	−155.235 54	−80.093 39	−75.199 89	36.2
B3P86/6-311+G(2d,2p)	−155.349 28	−80.186 73	−75.221 82	37.2
B3P86/6-311+G(2d,2p) (0 K)	−155.277 73	−80.112 04	−75.221 82	35.2
B3PW91/6-31+G(d,p)	−154.784 34	−79.811 47	−75.036 95	40.2
B3PW91/6-31+G(d,p) (0 K)	−154.712 06	−79.736 67	−75.036 95	38.6
B3PW91/6-311+G(2d,2p)	−154.825 14	−79.829 41	−75.058 69	39.5
B3PW91/6-311+G(2d,2p) (0 K)	−154.753 43	−79.754 83	−75.058 69	37.7
MB3LYP/6-31+G(d,p)	−154.752 43	−79.775 73	−75.037 72	38.3
MB3LYP/6-31+G(d,p) (0 K)	−154.680 65	−79.701 23	−75.037 72	36.6

based on B3LYP and MB3LYP. The MP2 method gives shorter distances yet than all the DFT methods.

There is no experimental measurement for activation energy of methyl abstraction from ethane by O(3P). It has been shown by Jursic[42] that a G1, G2, or G2MP2 computational approach calculates activation barriers for hydrogen abstraction from methane by O(3P) that are identical to the experimental value. This reaction bears similarity to the methyl abstraction from ethane in the sense that both reactions take place on a triplet potential energy surface, the reactants are a stable molecule and an oxygen atom in its ground state, and the products are two radicals. Therefore, we believe it is reasonable to assume that the G2 theory should perform well in this case too. Our calculated G2 activation barrier for the methyl abstraction from ethane by O(3P) is 44.5 kcal/mol. The activation energy for this reaction with the use of another method that is supposed to produce very accurate energy values, CBS-QB3, is 41.1 kcal/mol. The two results are within the error limits of the theoretical methods which are ∼3 kcal/mol. The HF/3-21G value is 57.5 kcal/mol, and HF/6-31G(d,p) calculates it to be 60.9 kcal/mol. Both of these values exceed the G2 result to a large extent. The MP2 method in conjunction with moderate size basis sets produces an energy barrier that is ∼4−7 kcal/mol higher than the G2 value. The DFT methods all calculate very similar values for the barrier, which are underestimates by ∼6−9 kcal/mol as compared to the G2 result.

Reactions of Higher Alkanes ($n = 1$, 2, or 3) with O(3P): $O(3P) + CH_2-(C_nH_{2n+1})_2 \rightarrow \cdot O-CH_2-(C_nH_{2n+1}) + \cdot C_nH_{2n+1}$. The key geometric parameters computed by HF and DFT methods of the transition-state structures for the reactions of propane, pentane, and heptane with O(3P) (in which the O(3P) attacks the central carbon atom) are presented in Table 3. In addition, the optimized Cartesian coordinates and calculated vibrational frequencies for the transition-state structures are available in the Supporting Information. The classical and vibrational adiabatic (zero-point corrected) reaction barriers obtained by HF and DFT methods are presented in Table 4.

There are several differences in the structures of the transition states for the reactions of higher alkanes as compared to the ethane case. First, the partially formed (O−C1) and partially broken (C1−C2) bonds are longer. Second, the oxygen atom is no longer aligned with the two carbon atoms. The O−C1−C2 angle is ∼160° as opposed to almost 180° in the case of ethane. In addition, in the case of pentane and heptane there is a considerable rotation around the C1−C1A bond, which results in a dihedral angle, C2−C1−C1A−C1B, of ca. −100° as opposed to 0° in the hydrocarbon chain. The cause of these differences is certainly the repulsion between the oxygen atom and the groups attached to the carbon atom that is being attacked by O(3P).

Despite the considerable differences in the geometrical parameters between the transition states of higher alkanes and that of ethane, the energy barriers for the reaction remain almost the same. HF/3-21G produces barriers of 58.4, 57.9, and 58.0 kcal/mol for propane, pentane, and heptane, respectively, as opposed to 57.5 kcal/mol for ethane. MB3LYP/6-31+G(d,p) calculated values for the barrier are 38.5, 36.3, and 36.5 kcal/mol for propane, pentane, and heptane, respectively, as opposed to 36.6 kcal/mol for ethane.

Discussion

In this work, we investigated one of the possible reaction pathways leading to the erosion of hydrocarbons by O(3P), namely, the chain breaking of a hydrocarbon caused by a single

TABLE 3: Structural Parameters (Å and deg) for the Transition State of the Reaction O(3P) + $CH_2-(C_nH_{2n+1})_2$ → $\cdot O-CH_2-(C_nH_{2n+1})+ \cdot C_nH_{2n+1}$, Where n = 1, 2, or 3

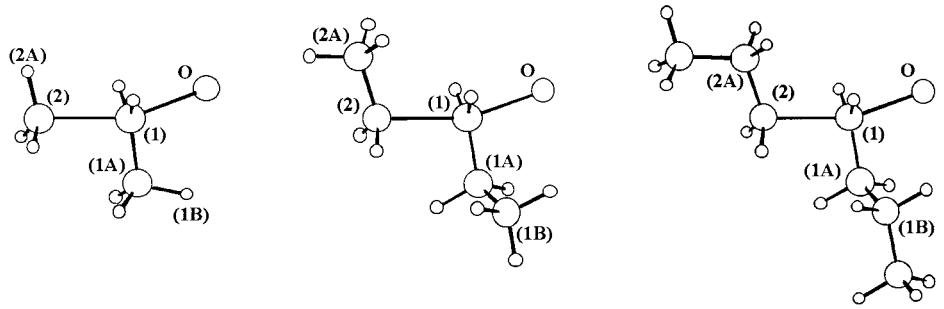

n	theory	r_{O-1}	r_{1-2}	a_{O-1-2}	a_{O-1-1A}	a_{1-2-2A}	$d_{2-1-1A-1B}$	$d_{O-1-1A-1B}$
1	HF/3-21G	2.119	2.500	162.9	100.5	99.5	178.7	−1.4
2		2.135	2.434	163.3	96.2	105.8	−105.6	71.9
3		2.141	2.444	163.2	96.4	106.5	−106.1	71.6
1	MB3LYP/6-31+G (d,p)	1.814	2.034	159.1	102.5	104.7	−173.9	6.8
2		1.843	2.033	160.1	99.1	109.1	−100.7	77.5
3		1.841	2.033	160.1	99.2	109.8	−100.7	77.6

TABLE 4: Total Energies (au) and Activation Barriers (kcal/mol) for the Reaction O(3P) + $CH_2-(C_nH_{2n+1})_2$ → $\cdot O-CH_2-(C_nH_{2n+1})$ + $\cdot C_nH_{2n+1}$, Where n = 1, 2, or 3

n	theory	E_{TS}	$E_{CH_2-(C_nH_{2n+1})_2}$	E_O	E_a
1	HF/3-21G	−191.904 75	−117.613 30	−74.393 66	64.1
	HF/3-21G (0 K)	−191.802 96	−117.502 34	−74.393 66	58.4
2	HF/3-21G(d)	−269.545 60	−195.251 56	−74.393 66	62.5
	HF/3-21G(d) (0 K)	−269.380 74	−195.079 37	−74.393 66	57.9
3	HF/3-21G(d)	−347.183 86	−272.889 77	−74.393 66	62.5
	HF/3-21G(d) (0 K)	−346.957 73	−272.656 46	−74.393 66	58.0
1	MB3LYP/6-31+G (d,p)	−194.037 59	−119.063 65	−75.037 72	40.0
	MB3LYP/6-31+G (d,p) (0 K)	−193.937 09	−118.960 72	−75.037 72	38.5
2	MB3LYP/6-31+G (d,p)	−272.617 75	−197.639 23	−75.037 72	37.1
	MB3LYP/6-31+G (d,p) (0 K)	−272.459 72	−197.479 77	−75.037 72	36.3
3	MB3LYP/6-31+G (d,p)	−351.193 19	−276.214 78	−75.037 72	37.2
	MB3LYP/6-31+G (d,p) (0 K)	−350.978 55	−275.998 94	−75.037 72	36.5

O(3P) attack. We used HF, DFT, MP2, G2, and CBS-QB3 theoretical methods to compute the energy barrier for such a reaction in ethane. The variation in values for the energy barrier was quite appreciable among the different methods. We believe that the most reliable estimates are the results obtained by the use of the G2 and CBS-QB3 methods, that is, ∼40−45 kcal/mol. We extended the investigation to the cases of propane, pentane, and heptane, using HF and DFT methods only. The results, that is, the reaction barriers for the reactions of the higher alkanes with O(3P), were very close to those of ethane, computed by the use of the same theoretical methods. This suggests that rather small molecules (in contrast to long polymer chains) can be used in modeling the reactions of O(3P) with materials without compromising the accuracy of the results. In addition, it seems that HF is likely to overestimate the value of the energy barrier for the reaction as compared to the G2 method, whereas DFT is likely to underestimate this value as compared to G2. Therefore, we believe that (for the sake of lower computational cost) these two methods can be used for the study of analogous reactions in similar systems in order to obtain an upper and a lower bound for the value of the energy barrier.

Experimental activation energies for the hydrogen abstraction reactions by O(3P) determined for various saturated hydrocarbons in the gas phase are 6.9, 4.5, and 3.3 kcal/mol for the primary, secondary, and tertiary hydrogen atoms, respectively.[43] The experimental energy barrier for the hydrogen abstraction by O(3P) from methane is 9.0−11.4 kcal/mol.[44] Thus, it is clear that hydrogen abstraction (and resulting subsequent reactions) is the low-energy pathway to hydrocarbon erosion by O(3P). Such reactions at low-impact energies in ground-based experiments might well be responsible for "carpetlike" surface morphologies similar to those observed in LEO. However, oxygen atoms in LEO collide with spacecraft surfaces at impact energies of ∼100 kcal/mol (the top of the Maxwellian distribution of speeds). We have shown that the collision energy available in LEO is more than enough to overcome the energy barrier (∼40−45 kcal/mol) for hydrocarbon chain breaking, therefore making an occurrence of such reactions in a LEO environment a definite possibility. For polyethylene, LEO erosion rates greatly exceed those of plasma asher experiments (see ref 17 for the description of plasma asher experiments). For those ground-based plasma asher experiments with O(3P) kinetic energy (∼1 kcal/mol at the energy distribution peak), which is much less than the activation energy, the same reaction (i.e., chain breaking) would be much less likely to occur. The hydrogen abstraction reactions would also be much less probable in plasma ashers. This would explain the great reduction in reaction probability in ground-based AO plasma asher experiments compared to AO in space. The relative contribution to the erosion rates of the two different mechanisms is not clear but should be highly dependent on AO energy, and thus experimental measurements of the polyethylene erosion rate's dependence on AO incident energy in the range of 0.1−10 eV would help to understand this.[45]

Although the ratio of H to C atoms in a linear hydrocarbon chain is 2:1, the ratio of hydrogen abstraction to chain-breaking sites is 1:1 (see Figure 1). This is due to the fact that the same carbon atom can be attacked from two sides. Therefore, we

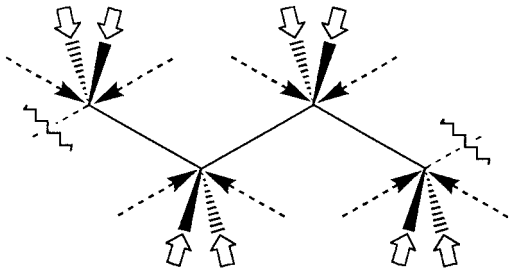

Figure 1. Possible sites for O(3P) attack on a hydrocarbon fragment. Short arrows indicate the hydrogen abstraction sites, and broken arrows indicate the chain-breaking reaction sites.

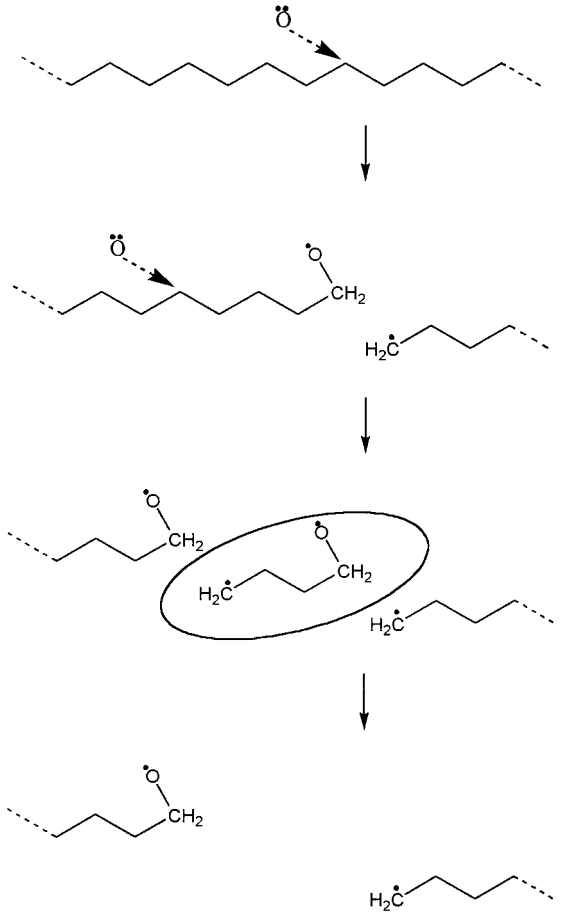

Figure 2. Proposed hydrocarbon erosion mechanism via chain-breaking reactions with O(3P).

speculate that from the geometrical point of view (in contrast to the energetical point of view) the two types of reactions might be equally probable.

The occurrence of chain-breaking reactions (in addition to hydrogen abstraction and all other related reactions) could greatly accelerate the erosion of hydrocarbons caused by O(3P). In Figure 2, we provide a scheme for the degradation of a hydrocarbon via chain-breaking reactions with O(3P). First, the polymer chain is broken by a single O(3P) attack. Second, the occurrence of another such reaction at an arbitrary site of the polymer chain disrupts the chain again, creating a loose fragment. In addition to various radical reactions at the surface, if the newly created fragment is small enough it could probably leave the surface altogether. Therefore, it takes only one step to disrupt the polymer chain and two steps to create a microscopic pit in it.

In Figure 3, we depict how the hydrocarbon chain could be disrupted via hydrogen abstraction, assuming one of the most

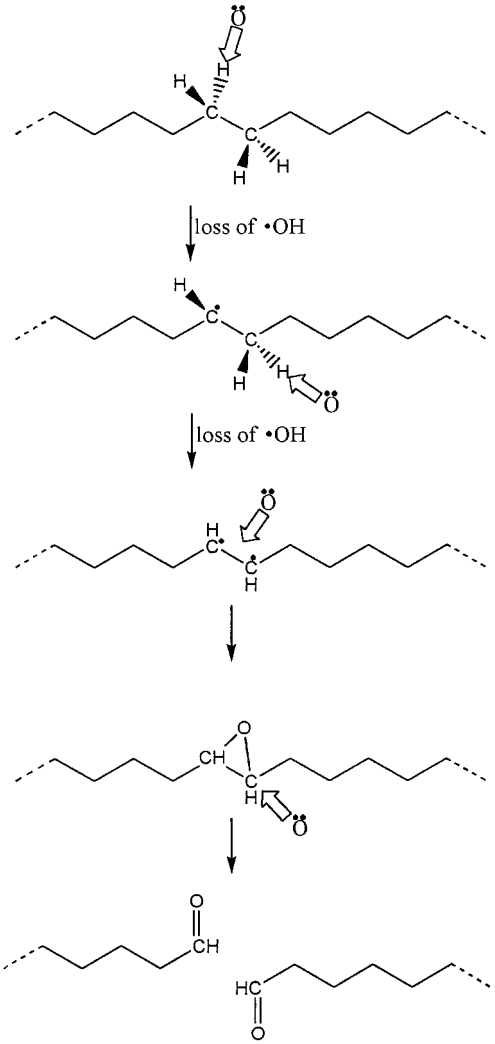

Figure 3. Proposed hydrocarbon erosion mechanism via hydrogen abstraction reactions with O(3P).

efficient pathways. First, a hydrogen atom is abstracted by O(3P), creating an OH radical (which, of course, could contribute to the degradation too, although we do not consider that here) and a radical site on the hydrocarbon chain. Second, O(3P) abstracts a hydrogen atom belonging to a carbon atom nearest neighbor of the carbon atom from the first step. Here, either a double bond between the two carbon atoms or two neighboring radical sites may be created. Third, O(3P) can react with either the double bond or the two neighboring radical sites, thus resulting in an epoxide. For the chain to be broken, the fourth oxygen atom has to attack one of the carbon atoms in the epoxide structure. Therefore, it takes at least four steps to break the hydrocarbon chain via this mechanism, whereas the same result could be accomplished in just one step via the chain-breaking pathway.

In this paper, we make no attempt to address the subsequent mechanisms leading to the ultimate reaction products which are associated with surface breakdown. We do assume that the initial step is a rate-limiting step, and we studied the mechanism associated with that.

Conclusions

In summary, we have calculated the activation barrier for a chain-breaking mechanism associated with O(3P) attack on a hydrocarbon chain. We have studied four small alkanes as

models of polyethylene. The magnitude of the activation barrier is similar for all these cases, making it a probable magnitude for longer polyethylenes too. Importantly, we have established that the calculated barriers (∼40−45 kcal/mol) are substantially less than the O(3P) kinetic energy available in LEO. Thus, chain breaking studied here is certainly an important candidate mechanism for contributing to polyethylene degradation in LEO. Moreover, chain breaking appears to be entropically advantageous over hydrogen abstraction mechanisms. If chain breaking is in fact an important contributor to degradation, this may affect the choice of strategies that would be employed to predict the erosion rates of materials in LEO at ground-based facilities. The type of study discussed in this paper can also be readily applied to similar polymers. For example, poly(tetrafluoroethylene) (PTFE) has a similar structure to that of polyethylene, differing only by the substitution of fluorine atoms for hydrogen atoms. The electronegativity of fluorine would seem, however, to preclude an abstraction mechanism similar to that which occurs in the case of hydrogen. This in fact would be an interesting study because a candidate mechanism to explain the degradation which occurs in this case is required. It may be that neither UV nor the synergy of UV and AO is responsible.[46−48] On the other hand, the results of this paper suggest the possibility that chain breaking by O(3P) is a contributing cause of degradation. Such studies would reveal whether chain-breaking mechanisms are equally important in other materials. Also, relative activation barriers might correlate with relative rates of degradation for different materials which share similar degradation mechanisms. (Experiments[49] have shown mass spectra of fragments emitted from the surface of fluorinated polymers under AO attack, which would be consistent with a chain-breaking mechanism although we do not assert that is the case.)

Finally, we point out that insofar as the chain-breaking mechanism might be important to degradation in space experiments, where O(3P) kinetic energy greatly exceeds our calculated E_a of ∼40−45 kcal/mol, it follows that for those ground-based plasma asher experiments with O(3P) kinetic energy (∼1 kcal/mol at the energy distribution peak), which is much less than the activation energy, the same reaction would be much less likely to take place. This would explain the great reduction in reaction probability in ground-based O(3P) plasma asher experiments compared to O(3P) in space.

Acknowledgment. We acknowledge the Maui High Performance Computational Center for the allocation of computational time. A.G. thanks the Burroughs-Wellcome Company for funding a Gertrude Elion Scholarship, administered by the Hunter College Chemistry Department. L.M. acknowledges an IBM Shared University Research (SUR) grant, a CUNY Research Award, a CUNY Collaborative Award, and a NASA JOVE/JAG grant.

Supporting Information Available: Optimized Cartesian coordinates and calculated vibrational frequencies for the transition-state structures of the reactions of O(3P) with ethane and higher alkanes. This material is available free of charge via the Internet at http://pubs.acs.org.

References and Notes

(1) *U.S. Standard Atmosphere, 1976*; NOAA-S/T 76-1562; National Oceanic and Atmospheric Administration, National Aeronautics and Space Administration, and the United States Air Force, U.S. Government Printing Office: Washington, DC, 1976.

(2) Banks, B. A.; de Groh, K. K.; Rutledge, S.; DiFilippo, F. J. *Prediction of In-Space Durability of Protected Polymers Based on Ground Laboratory Thermal Energy Atomic Oxygen*; NASA TM-107209; National Aeronautics and Space Administration: Washington, DC, 1996.

(3) Leger, L. J. *Oxygen Atom Reaction With Shuttle Materials at Orbital Altitudes*; NASA TM-58246; National Aeronautics and Space Administration: Washington, DC, 1982.

(4) Leger, L. J.; Visentine, J. T. *Aerosp. Am.* **1986**, *24*, 32.

(5) Hunton, D. E. Shuttle Glow. *Sci. Am.* **1989**, *261*, 92.

(6) Murr, L. E.; Kinard, W. H. Effects of Low Earth Orbit. *Am. Sci.* **1993**, *81*, 152.

(7) Reddy, M. R. *J. Mater. Sci.* **1995**, *30*, 281 and references therein.

(8) Banks, B. A. The Use of Fluoropolymers in Space Applications. In *Modern Fluoropolymers*; John Wiley & Sons: New York, 1997. See also references therein.

(9) Gregory, J. *On the Linearity of Fast Atomic Oxygen Effects*; NASA CP-3257; National Aeronautics and Space Administration: Washington, DC, 1993.

(10) Dooling, D.; Finckenor, M. M. *Material Selection Guidelines to Limit Atomic Oxygen Effects on Spacecraft Surfaces*; NASA TP-209260; National Aeronautics and Space Administration: Washington, DC, 1999. See also references therein.

(11) *Materials Degradation in Low Earth Orbit*; Srinivasan, V., Banks, B. A., Eds.; The Minerals, Metals and Materials Society: Warrendale, PA, 1990.

(12) Minton, T. K.; Nelson, C. M.; Brinza, D. E.; Liang, R. H. *Inelastic and Reactive Scattering of Hyperthermal Atomic Oxygen from Amorphous Carbon*; JPL Publication 91-34; Jet Propulsion Lab: Pasadena, CA, 1991.

(13) Banks, B. A.; Rutledge, S. K.; Paulsen, P. E.; Steuber, T. J. *Simulation of the Low Earth Orbital Atomic Oxygen Interaction with Materials by Means of an Oxygen Ion Beam*; NASA TM-101971; National Aeronautics and Space Administration: Washington, DC, 1989.

(14) Rutledge, S. K.; Banks, B. A.; DiFilippo, F.; Brady, J. A.; Dever, T.; Hotes, D. *An Evaluation of Candidate Oxidation Resistant Materials for Space Applications in LEO*; NASA TM-100122; National Aeronautics and Space Administration: Washington, DC, 1986.

(15) Garton, D. J.; Minton, T. K.; Alagia, M.; Balucani, N.; Casavecchia, P.; Volpi, G. G. Reactive Scattering of Ground-State and Electronically-Excited Oxygen Atoms on a Liquid Hydrocarbon Surface. *Discuss. Faraday Soc.* **1997**, *108*, 387.

(16) Kleiman, J. I.; Gudimenko, Y. I.; Iskanderova, Z. A.; Tennyson, R. C.; Morison, W. D.; McIntyre, M. S.; Davidson, R. Surface Structure and Properties of Polymers Irradiated with Hyperthermal Atomic Oxygen. *Surf. Interface Anal.* **1995**, *23*, 335.

(17) Koontz, S. L.; Albyn, K. A.; Leger, L. J. Atomic Oxygen Testing with Thermal Atom Systems: A Critical Evaluation. *J. Spacecr. Rockets* **1991**, *28*, 315.

(18) Tennyson, R. C. Atomic Oxygen Effects on Polymer-Based Materials. *Can. J. Phys.* **1991**, *69*, 1190.

(19) Chambers, A. R.; Harris, I. L.; Roberts, G. T. Reactions of Spacecraft Materials with Fast Atomic Oxygen. *Mater. Lett.* **1996**, *26*, 121.

(20) Iskanderova, Z. A.; Kleiman, J. I.; Gudimenko, Y. I.; Tennyson, R. C. Influence of Content and Structure of Hydrocarbon Polymers on Erosion by Atomic Oxygen. *J. Spacecr. Rockets* **1995**, *32*, 878.

(21) Frisch, M. J.; Trucks, G. W.; Schlegel, H. B.; Scuseria, G. E.; Robb, M. A.; Cheeseman, J. R.; Zakrzewski, V. G.; Montgomery, J. A., Jr.; Stratmann, R. E.; Burant, J. C.; Dapprich, S.; Millam, J. M.; Daniels, A. D.; Kudin, K. N.; Strain, M. C.; Farkas, O.; Tomasi, J.; Barone, V.; Cossi, M.; Cammi, R.; Mennucci, B.; Pomelli, C.; Adamo, C.; Clifford, S.; Ochterski, J.; Petersson, G. A.; Ayala, P. Y.; Cui, Q.; Morokuma, K.; Malick, D. K.; Rabuck, A. D.; Raghavachari, K.; Foresman, J. B.; Cioslowski, J.; Ortiz, J. V.; Stefanov, B. B.; Liu, G.; Liashenko, A.; Piskorz, P.; Komaromi, I.; Gomperts, R.; Martin, R. L.; Fox, D. J.; Keith, T.; Al-Laham, M. A.; Peng, C. Y.; Nanayakkara, A.; Gonzalez, C.; Challacombe, M.; Gill, P. M. W.; Johnson, B. G.; Chen, W.; Wong, M. W.; Andres, J. L.; Head-Gordon, M.; Replogle, E. S.; Pople, J. A. *Gaussian 98*, revision A.6; Gaussian, Inc.: Pittsburgh, PA, 1998.

(22) Mulliken is IBM proprietary software.

(23) Roothan, C. C. J. *Rev. Mod. Phys.* **1951**, *23*, 69.

(24) Pople, J. A.; Nesbet, R. K. *J. Chem. Phys.* **1959**, *22*, 571.

(25) McWeeny, R.; Dierksen, G. *J. Chem. Phys.* **1968**, *49*, 4852.

(26) Möller, C.; Plesset, M. S. *Phys. Rev.* **1934**, *46*, 618.

(27) Saebo, S.; Almlof, J. *Chem. Phys. Lett.* **1989**, *154*, 83.

(28) Pople, J. A.; Binkley, J. S.; Seeger, R. *Int. J. Quantum Chem., Symp.* **1976**, *10*, 1.

(29) Montgomery, J. A., Jr.; Frisch, M. J.; Ochterski, J. W.; Petersson, G. A. *J. Chem. Phys.* **1999**, *110*, 2822.

(30) Pople, J. A.; Head-Gordon, M.; Fox, D. J.; Raghavachari, K.; Curtiss, L. A. *J. Chem. Phys.* **1989**, *90*, 5622.

(31) Curtiss, L. A.; Jones, C.; Trucks, G. W.; Raghavachari, K.; Pople, J. A. *J. Chem. Phys.* **1990**, *93*, 2537.

(32) Curtiss, L. A.; Raghavachari, K.; Trucks, G. W.; Pople, J. A. *J. Chem. Phys.* **1991**, *94*, 7221.

(33) Curtiss, L. A.; Raghavachari, K.; Pople, J. A. *J. Chem. Phys.* **1993**, *98*, 1293.

(34) Scott, A. P.; Radom, L. *J. Phys. Chem.* **1996,** *100*, 16502.

(35) Becke, A. D. *J. Chem. Phys.* **1993,** *98,* 5648.
(36) Lee, C.; Yang, W.; Parr, R. G. *Phys. Rev. B* **1988,** *37,* 785.
(37) Perdew, J. P. *Phys. Rev. B* **1986,** *33,* 8822.
(38) Perdew, J. P. *Phys. Rev. B* **1987,** *34,* 7046.
(39) Perdew, J. P.; Wang, Y. *Phys. Rev. B* **1992,** *45,* 13244.
(40) Stephens, P. J.; Devlin, F. J.; Chabalowski, C. F.; Frisch, M. J. *J. Phys. Chem.* **1994**, *98*, 11623. MB3LYP is very similar to B3LYP defined in this paper, except that it uses the local correlation functional of Perdew and Wang (Perdew, J. P.; Wang, Y. *Phys. Rev. B* **1992**, *45*, 1324.) instead of the Vosko, Wilk, and Nusair functional.
(41) Foresman, J. B.; Frisch, A. *Exploring Chemistry with Electronic Structure Methods*, 2nd ed.; Gaussian, Inc.: Pittsburgh, PA, 1996.
(42) Jursic, B. S. *THEOCHEM* **1998,** *427,* 137.
(43) Andresen, P.; Luntz, A. C. *J. Chem. Phys.* **1980**, *72*, 5842.
(44) Gonzalez, C.; MacDouall, J. J. M.; Schlegel, H. B. *J. Phys. Chem.* **1990**, *94*, 7467 and references therein.
(45) For polyimide Kapton, some such experiments have been done (see ref 17). Note, however, that the chemical structure of this material is quite different from that of polyethylene, the material we address in this paper, although both materials have sometimes been referred to simply as "hydrocarbons". Different chemical structures in general imply different mechanisms, different activation energies, and different reaction rates.
(46) Koontz, S. L.; Leger, L. J.; Albyn, K. A.; Cross, J. Ultraviolet Radiation/Atomic Oxygen Synergism in Materials Reactivity. *J. Spacecr. Rockets* **1990**, *27*, 346.
(47) Rutledge, S. K.; Banks, B. A. *A Technique for Synergistic Atomic Oxygen and Vacuum Ultraviolet Radiation Durability Evaluation of Materials for Use in LEO*; NASA TM-107230; National Aeronautics and Space Administration: Washington, DC, 1996.
(48) Rutledge, S. K.; Banks, B. A.; Kitral, M. *A Comparison of Space and Ground Based Facility Environmental Effects for FEP Teflon*; NASA TM-207918/REV1; National Aeronautics and Space Administration: Washington, DC, 1998.
(49) Cazaubon, B.; Paillous, A.; Siffre, J. Mass Spectrometric Analysis of Reaction Products of Fast Oxygen Atoms-Materials Interactions. *J. Spacecr. Rockets* **1998**, *35*, 797.